INNOVATIONS

ITERATIVE MODEL RECONSTRUCTION: SIMULTANEOUSLY LOWERED COMPUTED TOMOGRAPHY RADIATION DOSE AND IMPROVED IMAGE QUALITY

D. Mehta, R. Thompson, T. Morton, A. Dhanantwari, E. Shefer

Philips Healthcare, Cleveland, USA

Abstract— **Computed Tomography (CT) scanner technology has progressed rapidly throughout the past decade, with major advances in CT x-ray detection, system speed, and image reconstruction that have resulted in a still-increasing number of novel CT clinical applications. Concomitant to this increase in clinical applications, CT technology has also experienced innovation to support the realization of high CT image quality while adhering to the As Low As Reasonably Achievable (ALARA) principal of radiation dose management. Notable among these innovations are the introduction of modular detector designs that are optimized for low-energy, low-noise data acquisition (e.g., NanoPanel Elite, Philips Healthcare) and the introduction of innovative reconstruction techniques (e.g., iDose[4], Philips Healthcare) that improve image quality at low-dose, and exhibit reconstruction times that fit within traditional CT workflow.**

The evolution to knowledge-based iterative reconstruction algorithms that utilize additional system information to enable significant CT radiation dose reduction and image quality improvement is the next step in CT technology innovation. Although these more advanced algorithms have been used in single-photon-emission computed tomography and positron-emission tomography for some time, their use in CT was historically limited by long, clinically unacceptable, reconstruction times.

Recently, IMR (Iterative Model Reconstruction, Philips Healthcare), combined with new computational hardware, has demonstrated simultaneous significant improvements in image-quality and significantly lower dose with reconstruction times of less than 5 minutes for a majority of reference protocols. Phantom tests demonstrate that IMR may simultaneously enable 60% – 80% lower radiation dose, 43% – 80% low-contrast detectability improvement, and 70% – 83% less image noise, relative to filtered back projection. Alternatively, IMR may enable 1.2x – 1.7x high-contrast spatial-resolution improvement; or 2.5x – 3.6x low-contrast detectability improvement; or 73 - 90% image noise reduction, relative to filtered back projection.

This article provides a review of the algorithm and its performance characteristics based on phantom studies.

Keywords— **Iterative Reconstruction, Knowledge-based, Model-based, IMR**

I. INTRODUCTION

During the last decade, technological advances have markedly enhanced and expanded the range of computed tomography (CT) clinical applications [1]. Consequently, physicians have ranked CT atop the list of innovations that have improved patient care. While the benefits of CT have been very well documented, increasing radiation doses to the population drew attention to the need for reducing radiation exposure from CT [2]. In response, the radiology community has worked to adhere to ALARA principles in CT imaging [3]. Working closely with the clinical community, dose management is simplified further with the advances in CT scanner technology [4]. Each stage of the imaging chain—from tube to detector—has been enhanced with innovative volume imaging technology and integrated with new dose management and reporting tools [5]. Novel reconstruction algorithms allow further opportunities to manage dose and improve image quality [6,7].

Filtered back projection (FBP) has been the industry standard for CT image reconstruction for decades. While it is a very fast and fairly robust method, FBP is a sub-optimal algorithm choice for poorly sampled data or for cases where noise overwhelms the image signal. Such situations may occur in low-dose or tube-power–limited acquisitions (e.g., scans of morbidly obese individuals). Over time, incremental enhancements were made to FBP to overcome some of its limitations. These improvements

continued until recently, when advances in computing performance made it possible to explore iterative reconstruction (IR), a completely different approach to image reconstruction. IR techniques, such as IMR (Iterative Model Reconstruction, Philips Healthcare)

attempt to formulate image reconstruction as an *optimization* problem i.e., IR attempts to find the image that is the "best fit" to the acquired data, while penalizing the noise [7].

Table 1 Evolution of CT reconstruction

Reconstruction	Potential Benefits	Description
Filtered backprojection		FBP has been the preferred algorithm for CT image reconstruction since its inception. This preference was attributed primarily to the ability of FBP to practically reconstruct images given the available computing resources; however, the limitations of FBP reconstruction have become more apparent as dose levels have been pushed to new lows in the spirit of imaging as low as reasonably achievable (ALARA).
Image-based Denoising [8]		Incorporating denoising in the image domain, these techniques were developed to produce reduced noise images, helping manage dose[6]. However, inability to address artifacts associated with significantly reduced doses, and limited image quality benefits, are becoming more apparent. Due to the reduced computational requirements, these techniques may achieve the reconstruction speeds of FBP. Current applications are limited to providing scanner agnostic, cost-effective solution; but at the expense of limited benefits.
Statistical / Hybrid Iterative Reconstruction		Incorporating statistics-model based denoising into raw and image data space these techniques are replacing FBP as the standard of CT reconstruction [6,9,10,11]. With significant noise reduction and artifact prevention, these techniques work well in helping manage dose while maintaining the image quality. Alternatively, Image quality benefits may be achieved. Combining dose management, with image quality improvements simultaneously may be limited with these approaches.
Model-based Iterative Reconstruction		Solving the reconstruction as an optimization process that incorporates forward-models (that model system geometry) in addition to statistics-models, these solutions take image quality and dose management further [12]. However, the long reconstruction times, restrictions to non-gated applications, and limited user flexibility, limit the routine applicability of these solutions.
Knowledge-based Iterative Model Reconstruction		Based on optimization processes similar to those used in model-based iterative reconstruction, solutions such as IMR (Philips Healthcare) enable model-based benefits that can be achieved routinely [7]. Increased computational requirements result in reduced recon speeds compared to statistical/hybrid approaches. However, newer hardware platforms can be designed to provide clinically acceptable reconstruction times.

II. EVOLUTION OF ITERATIVE RECONSTRUCTION

While different implementations of IR (image-based, statistical/hybrid-based, model-based, and knowledge-based) have been made commercially available by various vendors, their clinical value varies dramatically. There is continued debate in the scientific community with regard to the optimal implementation. Classification of reconstruction techniques based on their clinical results as well as objective phantom-based measurements provides a logical — and more meaningful — differentiation among these techniques. Also, the reconstruction times, flexibility and applicability to advanced modes such as ECG-gated scans, are other crucial components when evaluating the practical value of different IR implementations. The classification in this article is based on the value that reconstruction algorithms provide in terms of improving image quality, reducing radiation dose, and ease of integration into routine hospital workflow.

Knowledge-based iterative reconstruction algorithms such as IMR differ from FBP methods in that the reconstruction becomes an optimization process that takes into account the data statistics, image statistics, and system models[12]. These can be constrained optimization processes which still provide the user some amount of control over the desired image characteristics. Figure 1 gives a high-level overview of the IMR algorithm.
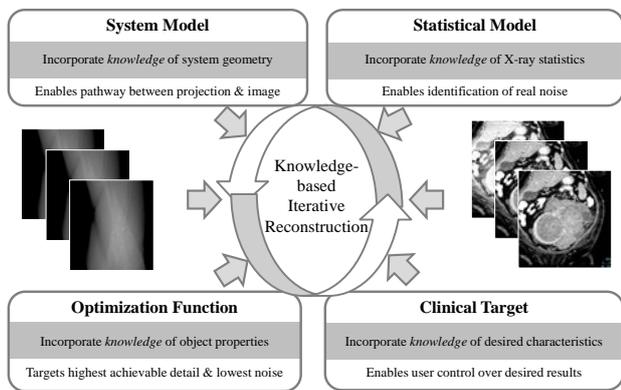

Fig. 1 IMR – Algorithm Overview

Very simplistically a cost function represents (a) the difference between an estimate of the data and the actual data that was acquired, and (b) a regularization term. Since, it can be expected that a noisy image will be a valid solution the difference between estimate and actual data, a constraint (regularization) is required. A constraint that enforces image smoothness would drive the optimization process to produce noise free data, and the level to which this is enforced can control the level of noise reduction. A smoothness constraint will take into account knowledge of the data statistic models. In other words, knowledge of the quantum noise statistics in the projection data could introduce bounds on the solution of the problem.

In addition, in the formulation of the cost function, there are known characteristics of the CT system that can additionally be used to target a desired resolution of the solution. For example, the achievable spatial resolution of the final image is driven by the detector sampling, angular sampling and system geometries. Spatial resolution can be maximized without the introduction of image artifacts by including this knowledge into the optimization process. Similar models for different system components and system physics can be introduced. Together, the careful consideration of the system properties allow for design of the cost function, allowing IMR to effectively control the image noise while maximizing spatial resolution at radiation doses that are significantly lower than those traditionally used with FBP reconstruction.

Algorithmic choices on a knowledge-based IR solution help overcome the motion sensitivity associated with traditional model-based solution, allowing for knowledge-based IR solutions to be used in advanced modes such as Cardiac CTA.

Furthermore, algorithmic optimizations of this knowledge-based solution combined with cutting edge reconstruction hardware leads to fast reconstruction times of less than 5 minutes for a majority of reference CT protocols, as can be seen in figure 2.
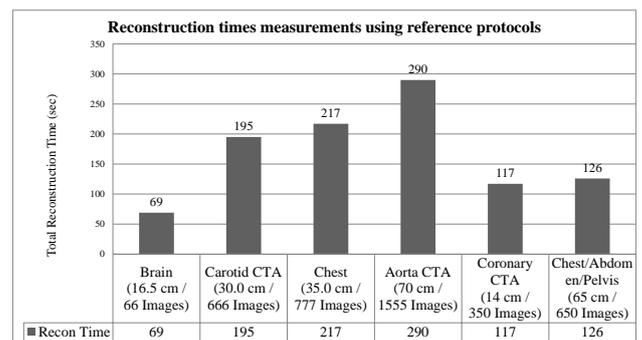
Fig. 2 Plots of IMR reconstruction time measurements for sub-set of reference protocols on a Philips Ingenuity Elite scanner.

III. PHANTOM TESTING

Image quality testing using standardized methods for objectively measuring noise, high contrast spatial resolution, CT number accuracy and CT number uniformity was conducted on phantoms to provide reproducible objective data. The parameters for testing were selected to provide denoising effects expected to be

appropriate for different clinical tasks. Additionally, tests for evaluating the performance of IMR with respect to dose reduction, and low contrast detectability (LCD) were conducted using test methods emerging in the industry as standardized approaches for such assessments.

Descriptions of the image quality metrics, phantom-based tests utilized for the IMR evaluation and their results are discussed in this section.

A. Image Noise

Image noise is a measure of statistical fluctuations in the image. It is a consequence of a variety of statistical processes that occur in the detection of x-rays by a CT system, but the dominant source is the quantum fluctuations in x-rays. An x-ray tube will not emit an exact number of x-rays over a given time period, but rather the number of x-rays will fluctuate around a mean value according to a Poisson distribution. After attenuation through the patient and detection at the detector, which are governed by further statistical processes, the measured data will contain noise which gets transferred into the image during reconstruction. Noise is measured by calculating the standard deviation of pixels in an region-of-interest (ROI) of a uniform section of a phantom.

A water phantom (water equivalent diameter = 30 cm) and the technique standardized in IEC61223-3-5 section 5.5 were utilized for the testing. To characterize the noise performance across the typical dose range used clinically, multiple acquisitions were performed to cover a range of 50 – 500 mAs, in 50 mAs increments. All other acquisition parameters were held constant at 64 x 0.625 collimation, 120kVp, 512 x 512 matrix and standard resolution. Thin-slices of 1.0 mm thickness were reconstructed using FBP (Filter B), iDose^4 (Filter B, Level 4 = mid-level & Level 6 = high-level) and IMR. IMR reconstructions were targeted for low-contrast visualization ("Image definition" = soft tissue, "noise reduction" = Level 3). Standard deviation of pixels was measured using a circular ROI with area 5000±200 mm^2, for the different reconstructions and dose levels, at the same phantom location. Results showed that noise reduction of up to 90 % was achieved with IMR, relative to FBP. Additionally, the noise performance stayed fairly constant, less than 10 HU, across the dose range tested. Figure 3 shows the noise versus dose measurements using the three reconstruction techniques.
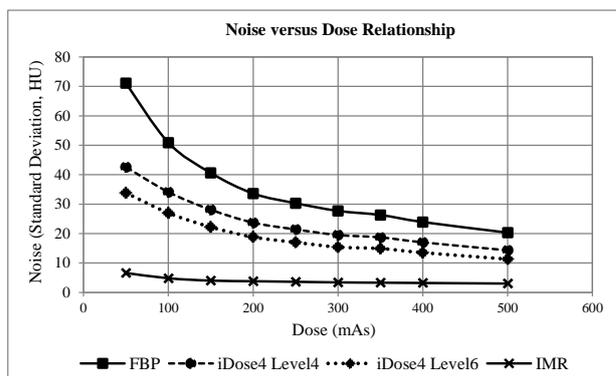

Fig. 3 Phantom images of same acquisition reconstructed using FBP (left) and IMR (right). Images demonstrate a 90.2% reduction in noise.

B. CT Number Accuracy

CT number accuracy is the ability of a CT system to accurately represent the CT number, expressed in Hounsfield Units (HU), in an image. The multi-pin layer of the Brilliance system phantom was utilized for the testing. The multi-pin layer contains pins of various materials (Teflon, Lexan, Acrylic, Teflon), within a water background. Acquisitions were performed across head & body protocols, and reconstructed using FBP (Filter B) and IMR. Measurements of the CT number (HU) was performed using a circular ROI, covering ¾th of the pin diameter. Results showed that when reconstructing the same data set with FBP and IMR, the CT number accuracy was maintained between reconstruction types. Table 2 summarizes the measurements.

Table 2 CT Number (HU) accuracy measurements

Object	FBP CT Number (HU) ± Noise (HU)	IMR CT Number (HU) ± Noise (HU)
Water	2 ± 14	2 ± 2
Polyethylene	51 ± 12	53 ± 2
Lexan	109 ± 12	111 ± 2
Acrylic	137 ± 11	137 ± 2
Teflon	916 ± 16	917 ± 5

C. High-contrast Spatial Resolution

High contrast spatial resolution is a measure of an imaging system's ability to preserve the spatial information in a high contrast object and accurately represent it in the image. It is expressed in terms of the modulation transfer function (MTF). Many factors influence the high contrast spatial resolution, including the design of the x-ray tube and detector, as well as the reconstruction algorithm. Traditional trade-offs between noise and spatial resolution in computed tomography exists via the reconstruction filter. In FBP, sharper filters can be used to produce images with high resolution, but

at the penalty of increased noise and reduced low-contrast. With IMR, high contrast spatial resolution is improved while simultaneously reducing noise.

The high contrast MTF was measured using a standardized technique (IEC61223-3-5: 5.6) on a CatPhan® 600 phantom, module CTP591 using the 50 micron tungsten wire. Acquisitions were performed at routine dose of 20.0 mGy, and low dose of 4.0 mGy. Additionally, high-res (small focal spot) acquisitions with similar dose parameters were performed. All other acquisition parameters (collimation, kVp, etc.) were held constant. Thin-slices of 1.00 mm thickness were reconstructed using FBP (Filter B), and IMR. IMR reconstructions were targeted for high-contrast (Image definition = Sharp, noise reduction = Level 3). The $MTF_{50\%}$ and image noise were measured.

Results showed 1.2x to 1.7x improvement in high-contrast resolution with 43% less image noise, simultaneously. The lower-bound captures the improvement when using IMR and low-dose (4 mGy), and the upper-bound when using IMR at routine-dose (20 mGy) when combined with the high-resolution acquisition mode. Figure 4 captures the noise and spatial resolution improvements.
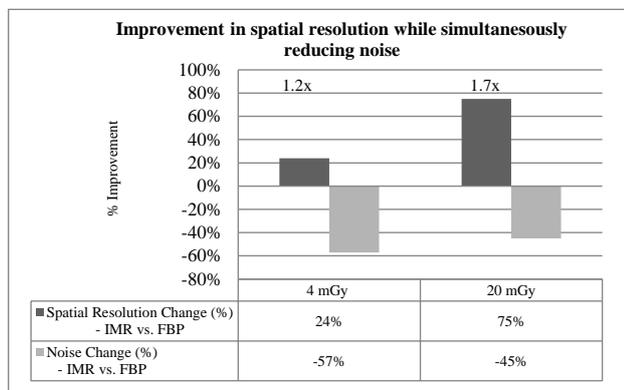

Fig. 4 Plots of image noise and high contrast spatial resolution improvements (%) with IMR, relative to FBP, at 4 mGy (left) and 20 mGy (right). Results demonstrate 1.2x to 1.7x improvement in spatial resolution, with noise reduction, simultaneously.

D. Low-contrast Detectability

The image quality metrics discussed thus far are properties of the imaging system alone. They represent the degree to which a CT scanner generates images which accurately represent various aspects of what is in the scanned object. Physical measurements, and mathematical analysis of those measurements, characterize image quality independently from how it might be perceived by a person looking at the image. Low contrast detectability (LCD), on the other hand, is a measure of a person's ability to perform a particular task: the detection of a low contrast object. LCD is influenced

to some degree by all of the image quality metrics discussed above, as well as the reaction of the human visual perception system to those factors. High noise may obscure the low contrast object in the noise and make it difficult for a human to perceive it. Poor spatial resolution may blur the object and blend it in with the background and poor uniformity or CT number accuracy may confound a person's ability to visualize a low contrast object. Due to the influence of noise, and the fact that the exact appearance of noise changes from one scan to the next, accurately capturing the influence of noise on LCD requires a statistical approach. In other words, LCD cannot be assessed from a single image, but rather an ensemble of images must be used to characterize the average performance. To assess the impact of IMR on low contrast detectability, it was measured by a method known as a human observer study. This is a new phantom and bench testing methodology that the industry is moving towards for assessing LCD [14]. In this method, a cohort of human test subjects is asked to perform a low contrast detectability task on a set of repeated scans of a phantom. The particular method employed is known as an alternative forced choice human observer test [15]. From the average ratio of correct responses, a quantity known as the detectability index can be calculated. The detectability index is a dimensionless quantity that characterizes the degree to which subjects can distinguish images with the low contrast object present from those with it absent. The detectability index ranges from 0, where subjects have no ability to distinguish the low contrast object, to higher values representing improvement in low contrast detectability. An alternative forced choice human observer study was used to show that IMR reduces noise in images without degrading low contrast detectability. The phantom used is a custom made low contrast phantom from the Phantom Laboratories. It is 20 cm in diameter, consisting of a Catphan-like shell, and a background plastic with CT number of approximately 45 HU at 120 kVp. It contains four low contrast pins with diameters of 3, 5, 7, and 10 mm and contrast levels of +14, +,7 +5 and , and +3HU respectively. Each pin is 20 mm long, and all four pins are located in the same z-position of the phantom. A significant improvement in LCD was measured for IMR compared to FBP. This can be seen with the following two types of scans:

Acquisitions were performed using 10 mGy to assess improvements at routine dose, and 4 mGy to assess improvements at low dose. All other acquisition parameters (collimation, kVp, etc.) were held constant. Reconstructions were performed using FBP (Filter B, and Filter C) and IMR. To assess performance characteristics across the IMR settings, reconstructions were performed using both low-contrast visualization, and high-contrast visualization, settings. Assessments in LCD were

performed by 36-observers, based on 200 image datasets each, using the human-observer method described above.

Results showed 2.5x to 3.6x improvement in low-contrast detectability. The lower bound captures the improvement with IMR at routine-dose and high-resolution optimized settings, and the upper-bound when using IMR at low-dose with low-contrast optimized settings. Figure 5 summarizes the IMR LCD results.

Fig. 5 Plots of LCD assessments using FBP & IMR, at 4 mGy (left) and 10 mGy (right). Results demonstrate 2.5x improvement in LCD at routine-dose of 10 mGy and 3.6x at low-dose of 4 mGy

E. Dose Reduction

Low-contrast detectability assessments similar to the methodology previously discussed were performed to assess the dose reduction capability of IMR. Multiple 120 kVp acquisitions were performed using 10 mGy, 4 mGy, and 2 mGy dose. Reconstruction of the routine-dose (10 mGy) was performed using FBP (Filter B), and the low-dose was performed using IMR. To assess performance characteristics across the IMR settings, reconstructions were performed using both low-contrast visualization, and high-contrast visualization, settings. All other reconstruction parameters were held constant (0.8 mm slice thickness, 512 matix). Assessments in LCD were performed by 36-observers, based on 200 image datasets each, using the human-observer method previously described.

Results showed that with low-contrast optimized settings IMR could achieve 80% lower radiation dose with an 80% improvement in low contrast detectability and 70% less image noise. This was achieved when using the low-contrast optimized settings of IMR. When the settings were optimized for high-contrast, IMR could achieve 60% lower radiation dose with a 43% improvement in low contrast detectability and 83% less image noise. Figure 6 summarizes the results.

Dose Reduction + Improved LCD + Lower Noise
(Low-contrast optimized IMR settings)

80% Lower Dose   80% Improved LCD   70% Lower Noise

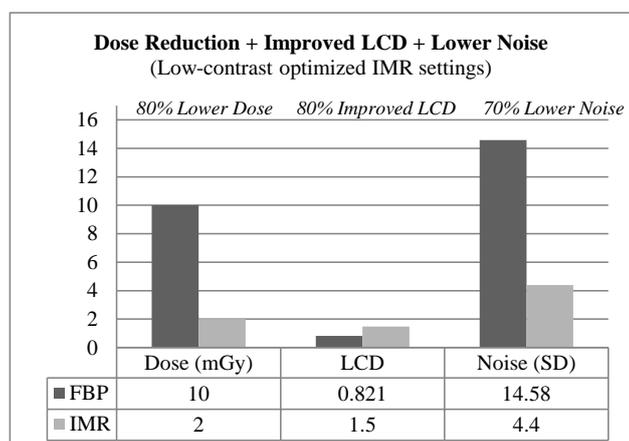|	Dose (mGy)	LCD	Noise (SD)
FBP	10	0.821	14.58
IMR	2	1.5	4.4

Fig. 6 Dose reduction assessments using human-observer studies, demonstrating 80% lower dose, with 80% lower LCD, with 70% lower noise.

F. Low Contrast Resolution

Low contrast resolution is a measure of the ability to distinguish a low contrast object from its background. Low contrast resolution is measured with a CatPhan® 600 module CTP515, with a viewing setting (window level & width) close to the CT number values of the low contrast pins. Low contrast resolution is usually expressed as the smallest visible pin at a specific contrast level, at the scanned $CTDI_{vol}$.

Acquisitions of the phantom were performed at 120 kVp, 10.4 mGy $CTDI_{vol}$,. Repeated assessment by multiple readers on 7 mm slices showed the median visualization of the 2 mm pins with 0.3 % contrast. Figure 7 demonstrates a sample image from the IMR LCD results.
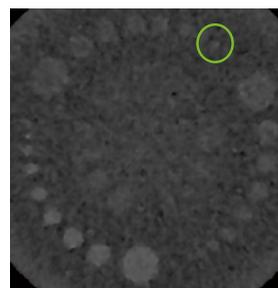
Fig. 7 Low contrast resolution of 2 mm contrast pin, at 0.3% contrast at 10.4 mGy $CTDI_{vol}$

IV. CLINICAL EXAMPLES

The clinical studies in figures 8-13 provide representative examples of the expected image quality and dose reduction capabilities that may be achieved with IMR. These are based on ongoing investigations at multiple clinical sites. In clinical practice, the use of IMR may reduce CT patient dose depending on the clinical task, patient size, anatomical location, and clinical practice. A consultation with a radiologist and a physicist should be made to determine the appropriate dose to obtain diagnostic image quality for the particular clinical task.

Chest CT at nearly the dose of chest x-ray

FBP   IMR

80 kVp, 10 mAs, 0.2 mGy, 8.2 mGy x cm, 0.11 mSv (k = 0.014)

Fig. 8 A Chest scanned on a Philips iCT at 0.11mSv (80 kVp, 10 mAs, 0.2 mGy, 8.2 mGy x cm) and reconstructed using FBP (left) and IMR (right). Study shows limited visualization of the Ground Glass Opacity on the FBP reconstructions. IMR significantly reduces noise and artifacts, revealing structural information. Courtesy of Cliniques Universitaires St-Luc, Brussels, Belgium.

Dose Reduction with Image Quality Improvement

FBP | IMR
Routine-dose scan | Low-dose scan
4.2 mSv | 1.6 mSv

120 kVp, 249 mAs, | 120 kVp, 93 mAs,
14.6 mGy, 277.4 mGy x cm, | 5.5 mGy, 104.5 mGy x cm,
4.2 mSv (k = 0.015) | 1.6 mSv (k = 0.015)

Fig. 9 An abdomen scanned on a Philips iCT at routine-dose of 4.2mSv (120 kVp, 249 mAs, 14.6 mGy, 277.4 mGy x cm) reconstructed with FBP (left), and the low-dose exam at 1.6mSv (120 kVp, 93 mAs, 5.5 mGy, 104.5 mGy x cm) reconstructed with IMR (right). IMR allows lower dose with improved image quality, simultaneously. Courtesy of Guangdong General Hospital, China.

Improved Low-contrast detectability

FBP   IMR

80 kVp, 500 mAs, 9.8 mGy, 170.5 mGy×cm, 2.5 mSv (k=0.015)

Fig. 10 An Abdomen scanned on a Philips iCT at 2.5mSv (80 kVp, 500 mAs, 9.8 mGy, 170.5 mGy×cm) and reconstructed using FBP (left) and IMR (right). Study shows limited visualization of lesions on the FBP reconstructions. IMR improves the low-contrast detectability. Courtesy of Guangdong General Hospital, China.

Improved low-contrast detectability

FBP | iDose[4] Level 5 | IMR
3 mm slice thickness | 3 mm slice thickness | 1 mm slice thickness

120 kVp, 300 mAs, 14.3 mGy, 1.8 mSv (k=0.0021)

Fig. 11 A brain scanned on a Philips iCT at 1.8 mSv (120 kVp, 300 mAs, 14.3 mGy) reconstructed with FBP at 3mm slice thickness (left), iDose[4] at 3 mm slice thickness (center), and IMR at 1 mm slice thickness (right). Study shows limited visualization of haemorrhagic lesions on FBP. IMR improves low contrast detectability. Courtesy of Cliniques Universitaires St-Luc, Brussels, Belgium.

Improved spatial resolution

FBP   IMR

100 kVp, 200 mAs, 8.8 mGy, 35.1 mGy×cm, 0.7 mSv (k=0.0021)

Fig. 12 A carotid CT angiogram on a Philips iCT at 0.7mSv (100 kVp, 200 mAs, 8.8 mGy, 35.1 mGy×cm), reconstructed using FBP (left) and IMR (right). Study shows limited resolution on FBP, at a given noise target. IMR significantly improves spatial resolution, and at the same time lowers noise. Courtesy of UCL, Belgium.

Improved image quality relative to previous generations of reconstruction

FBP   iDose⁴ Level 4   IMR

100 kVp, 110 mAs, 5.2 mGy, 67.1 mGy x cm, 0.9 mSv (k=0.014)
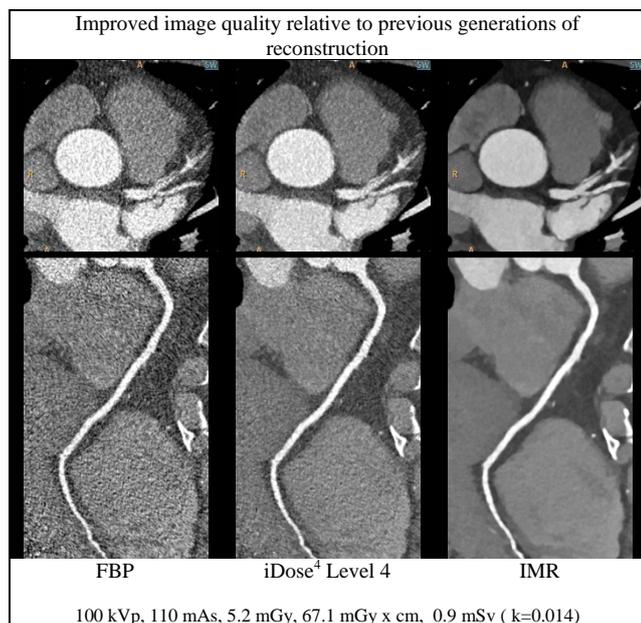
Fig. 13 An ECG-gated coronary CT angiogram scanned on a Philips iCT at 0.9 mSv (100 kVp, 110 mAs, 5.2 mGy, 67.1 mGy x cm) and reconstruction with FBP (left), iDose⁴ center, and IMR(right). Study shows limited visualization of soft-plaque on FBP. IMR improves spatial resolution, low-contrast, and noise characteristics. Courtesy of Amakusa Medical Center, Japan.

V. CONCLUSION

Phantom tests demonstrate that IMR may simultaneously enable 60% – 80% lower radiation dose, with 43% – 80% low-contrast detectability improvement, and with 70% – 83% less image noise, simultaneously; relative to filtered backprojection. Alternatively, IMR may enable 1.2x – 1.7x high-contrast spatial-resolution improvement; or 2.5x – 3.6x low-contrast detectability improvement; or 73 - 90% image noise reduction, relative to filtered backprojection. This is a major leap from capabilities of hybrid/statistical iterative reconstruction approaches.

Reconstruction speeds of less than 5 minute for a majority of the reference protocols, and applicability to non-gated and gated acquisitions, enables routine clinical use of IMR across a broad range of patients.

IMR is a paradigm shift in CT image quality. It emboldens a vision of expanding MDCT use, fueled by increasing clinical benefits and decreasing doses. This vision shows the way to provide information to increase diagnostic confidence and improve patient care.

ACKNOWLEDGMENT

We would like to thank our collaborators for sharing their clinical insights and the images demonstrating the

REFERENCES

1. ACR Appropriateness Criteria - http://www.acr.org/Quality-Safety/Standards-Guidelines/Practice-Guidelines-by-Modality/CT
2. Brenner DJ, Hall EJ (2007) Computed tomography: an increasing source of radiation exposure. N Engl J Med 357: 2277–2284
3. Image Wisely initiative - http://www.imagewisely.org
4. Vlassenbroek A, Mehta D, and Yanof J (2012), CT Radiation Dose: Philips Perspective, Radiation Dose from Multidetector CT, Radiology, Diagnostic Imaging, p. 617-632, Springer, ISBN 978-3-642-24534-3
5. Philips CT Dose Management tools: www.philips.com/ctdosemanagement
6. Kligerman S, Mehta D, Farnadesh M, Jeudy J, Olsen K, White C (2013), Use of a hybrid iterative reconstruction technique to reduce image noise and improve image quality in obese patients undergoing computed tomographic pulmonary angiography, J Thorac Imaging. Jan ; 28(1): 49-59
7. Brown K, Zabic S, Koehler T (2012), Acceleration of ML iterative algorithms for CT by the use of fast start images, Proc. SPIE 8313, Medical Imaging 2012: Physics of Medical Imaging, 831339 (February 23, 2012); doi:10.1117/12.911412
8. Lee S, Shima A, Singh S, Kalra MK, Kim HJ, Do S (2013), Co-registered image quality comparison in hybrid iterative reconstruction techniques: SAFIRE and SafeCT, Proc. SPIE 8668, Medical Imaging 2013: Physics of Medical Imaging, 86683G (March 6, 2013); doi:10.1117/12.2007525
9. Chen MY, Steigner ML, Leung SW, Kumamaru KK, Schultz K, Mather RT, Arai AE, Rybicki FJ (2013), Simulated 50 % radiation dose reduction in coronary CT angiography using adaptive iterative dose reduction in three-dimensions (AIDR3D), Int J Cardiovasc Imaging. Jun ; 29(5): 1167-75
10. Schabel C, Fenchel M, Schmidt B, Flohr TG, Wuerslin C, Thomas C, Korn A, Tsiflikas I, Claussen CD, Heuschmid M, Ketelsen D (2013), Clinical evaluation and potential radiation dose reduction of the novel sinogram-affirmed iterative reconstruction technique (SAFIRE) in abdominal computed tomography angiography, Acad Radiology Feb ; 20(2): 165-72
11. Marin D, Choudhury KR, Gupta RT, Ho LM, Allen BC, Schindera ST, Colsher JG, Samei E, Nelson RC (2013), Clinical impact of an adaptive statistical iterative reconstruction algorithm for detection of hypervascular liver tumours using a low tube voltage, high tube current MDCT technique, Eur Radiol. Jul 6.
12. Chang W, Lee JM, Lee K, Yoon JH, Yu MH, Han JK, Choi BI (2013), Assessment of a Model-Based, Iterative Reconstruction Algorithm (MBIR) Regarding Image Quality and Dose Reduction in Liver Computed Tomography, Invest Radiology, Aug ; 48(8): 598-606
13. ACR CT Accreditation Phantom Instructions - http://www.acr.org/~/media/ACR/Documents/Accreditation/CT/PhantomTestingInstruction.pdf
14. COCIR Press Release - CT Manufacturer's Voluntary Commitment Regarding CT Dose: http://www.cocir.org/site/fileadmin/Position_Paper_2013/COCIR_CT_MANUFACTURER_Commitment_2013_Status___Update_22_March_2013.pdf

15. Barrett HH, Myers KJ (2003), Foundations of Image Science (Wiley Series in Pure and Applied Optics), Wiley-Interscience; 1 edition, ISBN-10: 0471153001

Contacts of the corresponding author:

Author: Dhruv Mehta
Institute: Philips Healthcare
Street: 595 Miner Road
City: Highland Heights, Ohio
Country: USA
Email: Dhruv.Mehta@Philips.com